Topic Introduction

Spatial Light Modulator Microscopy

Volodymyr Nikolenko, Darcy S. Peterka, Roberto Araya, Alan Woodruff, and Rafael Yuste

The use of spatial light modulators (SLMs) for two-photon laser microscopy is described. SLM phase modulation can be used to generate nearly any spatiotemporal pattern of light, enabling simultaneous illumination of any number of selected regions of interest. We take advantage of this flexibility to perform fast two-photon imaging or uncaging experiments on dendritic spines and neocortical neurons. By operating in the spatial Fourier plane, an SLM can effectively mimic any arbitrary optical transfer function and thus replace, in software, many of the functions provided by hardware in standard microscopes, such as focusing, magnification, and aberration correction.

INTRODUCTION

Laser-scanning microscopy, such as confocal or two-photon fluorescence, has revolutionized the life sciences by making it possible to image biological tissues with high resolution under physiological conditions. Laser scanning is most often performed either with a pair of galvanometer mirrors, which steer the beam by rotating mirrors, or by acousto-optic modulators, which deflect the beam by diffraction caused by sound-induced changes in the refractive index. In these scanning modes, the image is reconstructed by sequentially moving the laser beam point by point and line by line across the sample in raster fashion. The drawback of this approach is that the temporal resolution is limited by the finite response time of the scanners. Even if it were possible to increase the scanning speed of the devices, a more fundamental limitation arises. Specifically, to maintain adequate fluorescence signal with the shorter dwell times per pixel (i.e., the time during which the beam remains at a certain point in the sample and collects optical signals from that point), it is usually necessary to increase the laser intensity. However, the rate of signal acquisition is limited by the number of chromophore molecules present and how often they can be excited (i.e., the duty cycle per lifetime in the case of fluorescence). This implies that even in the complete absence of photodamage, excitation intensity cannot be continually increased to achieve faster scanning or shorter dwell times because, regardless of the excitation power, the chromophores or fluorophores cannot produce more than a certain number of excitation–emission cycles per unit time. Thus, the signal cannot be made stronger by increasing the power because it is effectively saturated (Koester et al. 1999; Hopt and Neher 2001).

A logical way to overcome this second limitation is to parallelize the excitation process and use a scheme that can excite and acquire signals from multiple points of the sample at the same time. Traditional wide-field illumination does exactly that (although it is subject to other problems such as limited spatial resolution and blurring caused by cross talk between adjacent pixels). However, wide-field illumination is not a practical option for nonlinear optical methods such as two-photon fluorescent microscopy because existing ultrafast pulsed laser sources do not provide enough power to excite the whole field of view simultaneously.

Adapted from *Imaging: A Laboratory Manual* (ed. Yuste). CSHL Press, Cold Spring Harbor, NY, USA, 2011.

Cite this introduction as *Cold Spring Harb Protoc*; 2013; doi:10.1101/pdb.top079517

Diffractive Spatial Light Modulators

Although ultrafast lasers cannot illuminate the entire field, they are powerful enough to illuminate many points of interest at the same time. The difficulty is efficiently redistributing the light to only the areas that are of interest. Phase-only SLMs are ideally suited for this task, and they can dynamically adjust the number and location of active beamlets that can be used for imaging and photostimulation. Phase-only SLMs usually use a matrix of nematic liquid crystals similar to those used in multimedia projectors. However, in contrast to creating an image by masking certain pixels, phase-only SLMs take advantage of the wave properties of light and essentially work as a computer-controlled diffraction grating in which each pixel introduces different phase delays instead of modulating the intensity of passing light. That, in turn, leads to the creation of an image in the far field in a manner similar to classical Fraunhofer diffraction. The power of this approach is that almost any arbitrary pattern of intensity distribution can be created with minimal loss of power. This differs from the situation in which pixels are simply masked such as with digital micromirror devices (DMDs) (Wang et al. 2007). It is important to emphasize that if intensity modulators, such as DMDs, create illumination patterns by removing light, phase-only SLMs work by redistributing it. This redistribution of light leaves practically all of the power available, making it possible for nonlinear imaging modalities, such as two-photon absorption or second-harmonic imaging, to operate.

IMAGING SETUP

Adding a diffractive SLM to an existing microscope is a straightforward process. The SLM is a single small element, which is placed in the optical path, and can be positioned at almost any point before the objective lens, but ideally it should be on the plane that is optically conjugated to the back aperture of the objective. Existing laser-scanning systems can be easily modified to work with a diffractive SLM by placing the SLM on the plane that is conjugated to the existing scanners (i.e., the galvanometer mirrors) via a simple telescope.

Figure 1 illustrates the optical design of the SLM microscope used in our laboratory. A full description of the components used in the system can be found in Nikolenko et al. (2008). Here the design and logic of the SLM microscope are summarized. The elements of the optical pathway are listed approximately in the functional order of signal propagation. The numbered items below correspond to the numbers in Figure 1. Individual mirrors are not numbered, and unless otherwise noted, EO3 dialectical mirrors from Thorlabs, Inc. were used. These were optimized for the near-infrared (NIR) region (700–1200 nm) and did not introduce noticeable pulse broadening.

1. The source of illumination is an ultrafast, pulsed (mode-locked) laser, the Chameleon Ultra from Coherent, Inc.
2. The Pockels cell (Conoptics model 350–160) is controlled by a data acquisition board through a high-voltage driver (275 linear amplifier; Conoptics, Inc.).
3. A beam-sizing and reshaping telescope, which also works as a spatial filter if a pinhole (item 3b) is placed at the plane of focus of the first lens (3a) and the second lens (3c), recollimates the beam. We use standard BK7 thin plano-convex lenses with antireflection coating optimized for NIR (Thorlabs, Inc.). By choosing different lenses and placing them at the corresponding focal distances from the pinhole (item 3b), it is possible to change the size of the output beam without the need for additional realignment. It is convenient to use a lens kit from Thorlabs, Inc. (e.g., LSB01-B) to have the freedom to adjust the size of the beam easily. It is also convenient to mount lenses on flip mounts (e.g., model FM90; Thorlabs, Inc.), which makes it easy to reconfigure the optical path. Low-profile flip mounts (e.g., model 9891; New Focus) are also very convenient, and we use them in other parts of the optical path.
4. A polarizing half-wave plate (AHWP05M-950 achromatic λ/2 plate, 690–1200 nm; Thorlabs, Inc.) is mounted on a rotational mount (model PRM1; Thorlabs, Inc.). Rotating the half-wave plate rotates the plane of polarization to turn the diffraction of the SLM "on" or "off" (our liquid-

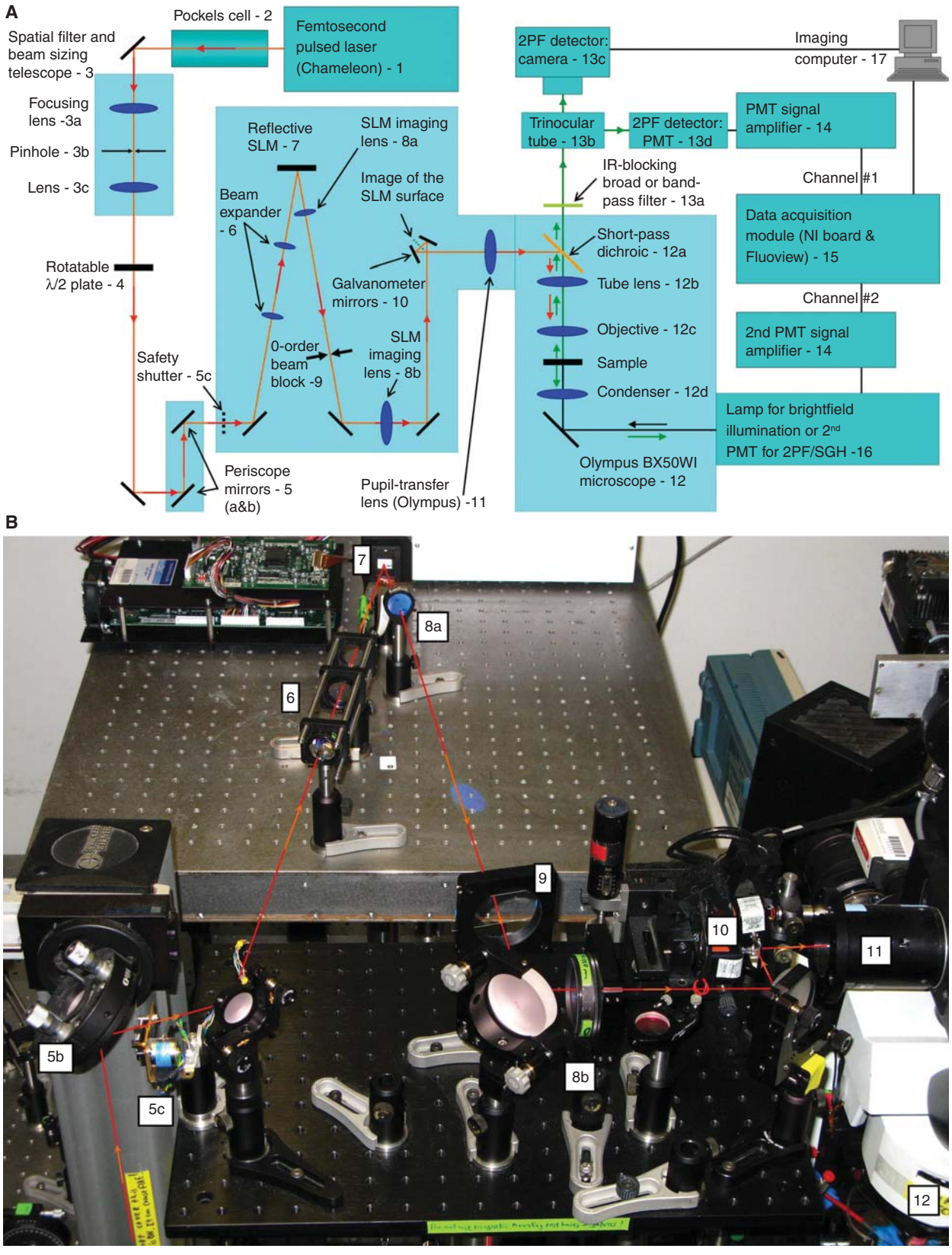

FIGURE 1. Optical design of an SLM microscope. (*A*) Optical diagram of the SLM microscopy system used in our laboratory. (*B*) Photograph of a portion of our SLM microscopy system. Red lines illustrate the laser excitation pathway. (Modified, with permission, from Nikolenko et al. 2008.)

Cite this introduction as *Cold Spring Harb Protoc*; 2013; doi:10.1101/pdb.top079517

crystal SLM is fully sensitive to polarization). When off, the SLM works as a passive mirror and allows regular scan mode imaging using galvanometer scanners (for high-resolution calibration images).

5. Periscope mirrors (5a and b): When using an upright microscope, it is convenient to bring the light from the plane of the optical table up to the "second floor"—that is, a raised breadboard with other optical elements that have to be in the vicinity of the input port of the upright microscope. A shutter (item 5c) is used to block the laser light when there is no scanning of the sample. Alternatively, the Pockels cell or the SLM could block the beam.
6. A secondary beam-resizing telescope, which is similar to item 3 and is made from a pair of thin plano-convex lenses, is desirable. The main function of this telescope is to make the laser beam large enough to fill the aperture of the SLM (0.7-in chip). This enables all of the available pixels to be used and spreads the power across a larger area to avoid damage to the SLM by the laser. This telescope is not absolutely required because its function can be fulfilled by the telescope in item 3, although it is convenient to have.
7. The diffractive SLM used is a model HEO 1080 P (HOLOEYE Photonics), configured to work in the reflection mode. It provides high-definition television resolution (1920×1080 pixels) and comes with simple software to compute the phase mask. To avoid distortions, it is important to minimize the angle of reflection for the SLM.
8. The second SLM telescope is arranged such that the surface of the SLM is conjugate to an intermediate image, which is itself conjugated to the back aperture of the microscope objective through the microscope's pupil transfer and tube lens. This same plane is also occupied by the galvanometer scanning mirrors (item 10), which are left from the original Olympus FluoView system. The first lens (item 8a) is a model LA1906-B, $F = 500$ mm (1-in. diameter; Thorlabs, Inc.). The second lens (item 8b) is larger (model LA1417-B, $F = 150$ mm [2-in. diameter]; Thorlabs, Inc.) to accommodate the full range of scanning angles necessary for the full field of view. To save space, the mirror (also 2-in. diameter) is placed between the lenses. The ratio of the telescope ($\sim$1:3) shrinks the beam and increases the deflection angles to match the range of angles expected by the scan lens of the microscope imaging port. The relative distances are important for matching the optical planes; thus, in its current configuration, the distance between the SLM (item 7) and the first lens (item 8a) is 90 mm, the total distance between lenses (8a) and (8b) is 650 mm (the sum of focal distances for telescope configuration), and the total distance between the second lens (8b) and the plane of galvanometers (10) is $\sim$190 mm.
9. The zeroth-order beam block allows only the diffracted (first-order diffraction) beam to reach the sample. The block is made from a small piece of metal foil glued to a thin glass cover slide. The element is mounted onto a flip mount (model FM90; Thorlabs, Inc.) for quick reconfiguration between actively using the SLM for multiplexed excitation, or using it as a passive mirror, when the diffraction is turned off by the half-wave plate (for high-resolution standard imaging).
10. Galvanometer scanning mirrors (Olympus FV200 system): Although separate mechanical scanners are not necessary for an SLM microscope, they provide additional flexibility to our system and were already present in our microscope. Standard Olympus FluoView software is used for slow high-resolution imaging, which is used for calibration purposes.
11. The scan (or pupil transfer) lens is a standard part of the Olympus FluoView system (FVX-PLIBX50/T). In combination with the microscope tube lens (item 12b), it forms a telescope and images the plane of galvanometers (and therefore, also the plane of the SLM chip) onto the back aperture of the microscope objective.
12. The Olympus BX50WI upright microscope is used without significant modifications. A dichroic mirror (item 12a; Chroma Technology) reflects excitation (NIR) light toward the sample and transmits visible fluorescence from the sample to the detector.
13. A short-pass (IR-block) filter or a combination of an IR-block and a band-pass filter (Chroma Technology) is used to reject scattered excitation light and to detect the signal within a chosen spectral region. The trinocular tube (item 12b; Olympus FV3-LVTWI) allows switching between two imaging ports, either multibeam SLM imaging with a camera (item 13c; Hamamatsu Orca

C9100-12 cooled electron-multiplying charge-coupled device [EMCCD] camera) or single-beam whole-field-of-view-scanning imaging using a photomultiplier tube (PMT) (item 13d; Hamamatsu H7422-40P cooled GaAs PMTs).

14. The signal amplifier (model PE 5113 preamplifier; Signal Recovery AMETEK Advanced Measurement Technology), used in combination with a current-to-voltage converter (a passive 5-kΩ load resistor in the simplest case), converts signals into a convenient range of voltages for digitizing.
15. The data-acquisition system is controlled by Olympus FluoView scanning software. The signal from the PMT is digitized by the FV 200 data-acquisition module. In certain situations, generic data acquisition cards (e.g., PCI 6259; National Instruments) and custom software are used.
16. Alternatively, the optical signal can be detected in a transmissive configuration. In our setup, a separate PMT is installed after the microscope condenser and detects either the second channel in two-photon fluorescence (different color) or the second-harmonic generation (SHG) signals. It is possible to install a camera in this pathway for multibeam imaging of transmissive SHG signals.
17. The computer receives images from the camera and/or digitizes PMT signals. The computer is also used to control excitation intensity via the Pockels cell. Our setup uses three computers with their software synchronized by through-the-lens triggers.

Phase-Mask Computation

Most algorithms for phase-mask computation are based on the fact that the phase-mask and far-field diffraction patterns are related through the Fourier transform (see Fig. 2 for a detailed explanation). Commercial software (e.g., from HOLOEYE Photonics) is available for computing phase masks, but

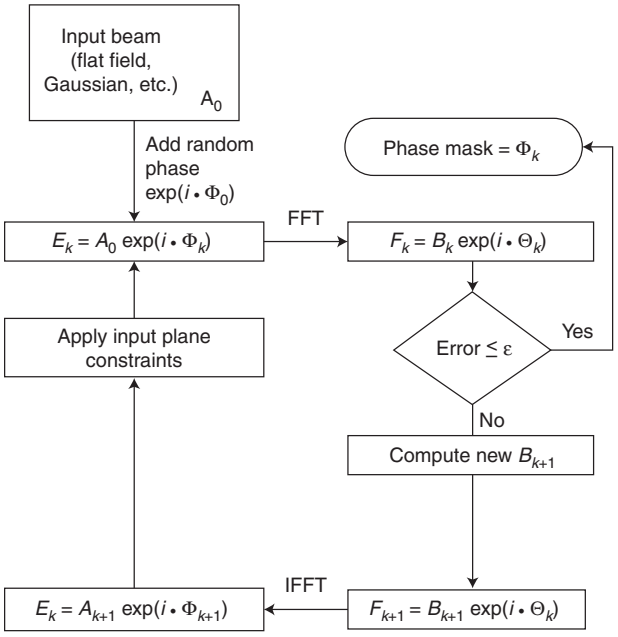

FIGURE 2. SLM phase-mask formation. The algorithm starts with the known intensity distribution of the laser and then adds a random phase (which speeds convergence), generating E_k. It then computes the spatial fast Fourier transform (FFT), F_k, and compares the computed image with the desired image. If the error exceeds a threshold, the amplitude, but not the phase, is modified to match the desired image better. An inverse fast Fourier transform (IFFT) is then performed, and constraints applied, such as phase quantization, giving rise to a new input field, and the cycle begins again. This description is deliberately nonspecific about the comparison process and modification because the optimal implementation critically depends on the physical parameters of the system (such as SLM resolution and desired deflection angles). More complete information on the variety of algorithms can be found in Kuznetsova (1988) and Bauschke et al. (2002). (Reprinted, with permission, from Nikolenko et al. 2008.)

Cite this introduction as *Cold Spring Harb Protoc*; 2013; doi:10.1101/pdb.top079517

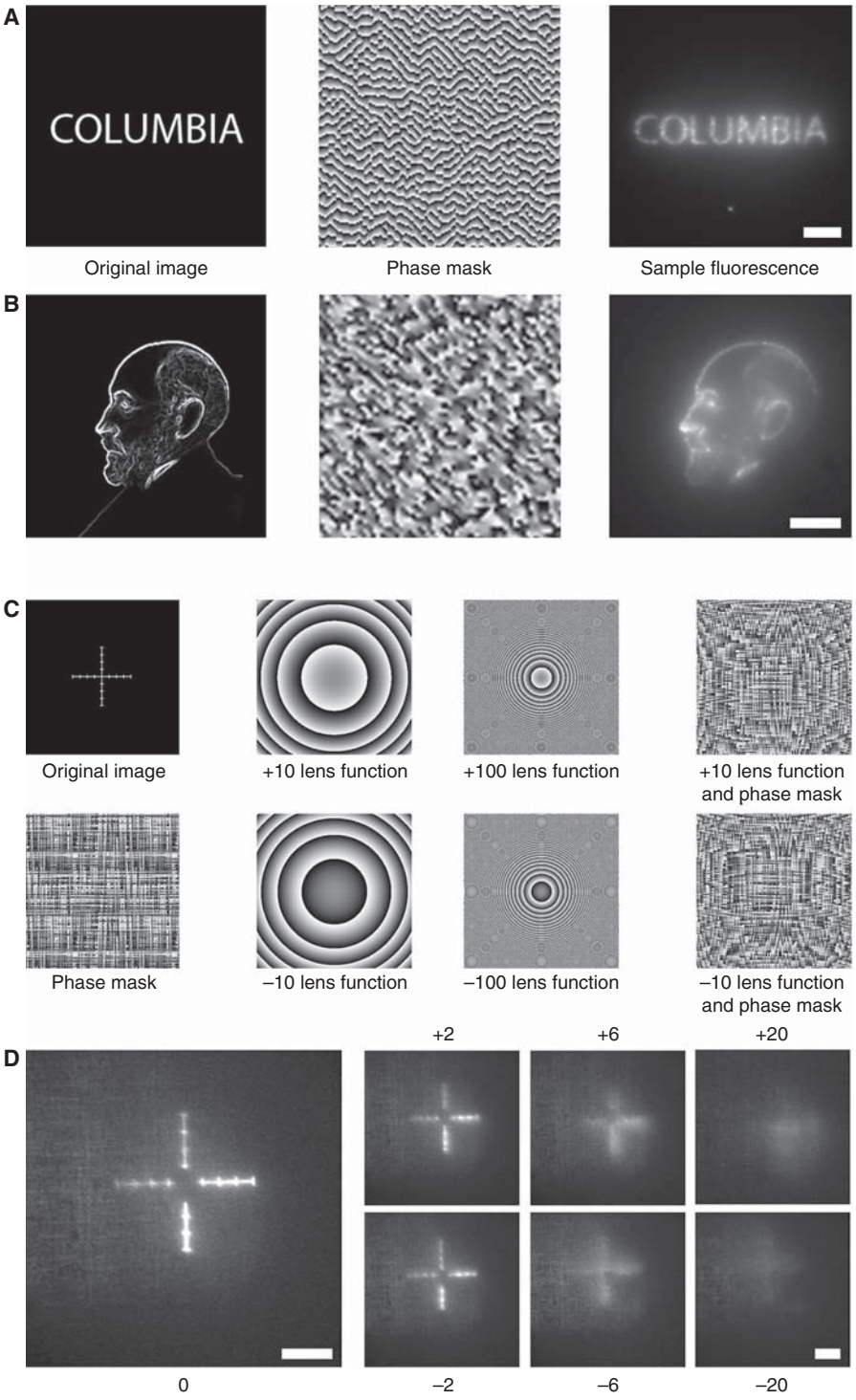

FIGURE 3. SLM light patterning and depth focusing. Imaging samples from an agarose gel saturated with Alexa Fluor 488 fluorescence indicator to test the efficiency of two-photon excitation. Images were acquired using a 60× 0.9-numerical-aperture (NA) objective. Scale bar, 20 µm. (*A*) A simple binary bitmap pattern (COLUMBIA) was uploaded into the SLM software, and the phase mask obtained is shown in the *middle* panel. Grayscale corresponds to a phase shift from 0 to 2π. The resulting two-photon fluorescence image of the sample acquired with the CCD is shown in the *right* panel. These data also show that liquid-crystal-based diffractive SLMs can withstand illumination by a powerful, pulsed mode-locked ultrafast laser and can be used effectively for structured nonlinear illumination. (*B*) Complex grayscale patterns can be used to program the SLM. A stylized picture of Santiago Ramón y Cajal, based on a historical photograph, was used. The panels are similar to those in (*A*). (*C*) Focusing with an SLM. The SLM software allows additional optical functions to be applied on top of the phase mask. (*Legend continues on following page.*)

there are circumstances in which it is valuable to write custom software that computes the phase pattern using generic algorithms based on iterative-adaptive algorithms (Fig. 2).

To show the ability of SLM microscopy to form arbitrary complex patterns, a series of tests were performed (Fig. 3). Binary (Fig. 3A, left panel) and grayscale patterns (Fig. 3B, left panel) were used as test images to be formed by diffractive SLM. The algorithm calculated the corresponding phase masks to be uploaded to the SLM (Fig. 3A,B, middle panels). Grayscale tones here have a meaning different from the imaging plane: White corresponds to 0 phase delay at that pixel, and black corresponds to a 2π phase shift (the whole wave) of the wave front at that point. These phase masks form diffraction images on the sample, which are shown in the right panels of Figure 3A and B. The optical signal in these images is actually the two-photon fluorescence that was generated in the sample of agarose gel infused with a fluorescent dye. These images were acquired by a camera and show the power of the nonlinear imaging approach with its inherent three-dimensional (3D) sectioning property. The relatively thick sample (i.e., fluorescent gel) represents one of the most challenging imaging scenarios with respect to contrast because every point of the sample is capable of generating fluorescence. With linear (one-photon) excitation, the image would be very blurry because linear excitation causes points of the sample both above and below the point of interest (on the focal plane) to fluoresce. To make the image usable, either deconvolution or confocal detection would be necessary.

Focusing with an SLM

Figure 3, C and D, shows another useful property of the SLM: 3D focusing. The SLM works as a universal modulator of the phase of light waves, so it can change the axial position of patterns by convolving phase masks with corresponding lens function. In fact, lenses simply convert plane waves into a spherical one, in a manner analogous to a physical thin lens (Fig. 3C, two middle panels). By varying the optical strength of the lens function, it is possible to shift the excitation pattern in the axial dimension in the sample (Fig. 3D). Moreover, any SLM that changes the phase of light can be used as a universal motionless scanner because, in principle, almost any complicated 3D pattern of illumination can be created by an appropriate phase mask.

APPLICATIONS OF SLM MICROSCOPY

Two-Photon Activation of Multiple Dendritic Spines

SLM microscopy has been used to study neurons and their dendritic spines. This work complements (and is in excellent agreement with) experiments using diffractive SLM microscopy for one-photon photoreleasing (uncaging) of glutamate (Lutz et al. 2008). The system described here uses two-photon photostimulation to uncage glutamate-activating neurons and dendritic spines to provide high spatial resolution of photostimulation. In an extension of single-spine uncaging experiments (Araya et al. 2006b, 2007), a two-photon laser is used here to simultaneously stimulate several dendritic spines by uncaging glutamate near their heads (Fig. 4A). Whole-cell electrodes were used to record the somatic membrane potential of pyramidal neurons in slices bathed with 2.5-mM 4-methoxy-7-nitroindolinyl-

FIGURE 3. (*Continued*) In this example, a lens function was used to shift the focus of excitation in the axial dimension. The original image and its corresponding phase mask as well as the lens phase function alone and added to the original phase mask are shown. The −10, −100, +10, and +100 are arbitrary units used by the software to indicate correspondingly a diverging or converging lens function and its relative optical strength. Note that increasing the optical strength of the lens function created by the SLM corresponds to a faster change of phase from the center to the edges of the SLM (rings of 2π phase reversal are spaced close together). (*D*) Two-photon fluorescence image of the test pattern acquired with the CCD camera. The virtual focus plane is moved away in both directions from the camera's imaging plane using a lens function of corresponding strength. A 40× 0.8 NA objective was used. Scale bars, 50 μm. These data illustrate that SLMs can be used as universal scanners that do not require moving parts. (Modified, with permission, from Nikolenko et al. 2008.)

 Cite this introduction as *Cold Spring Harb Protoc*; 2013; doi:10.1101/pdb.top079517

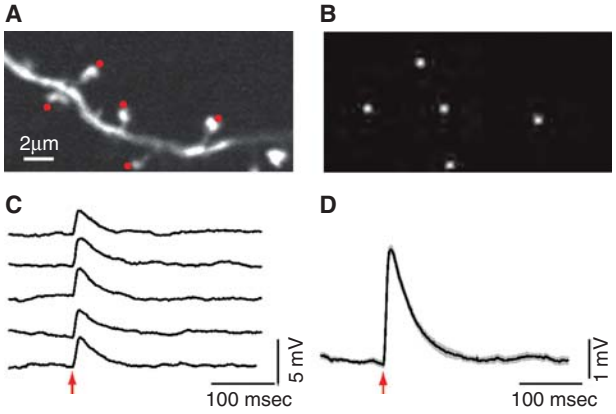

FIGURE 4. Simultaneous glutamate uncaging on multiple dendritic spines using an SLM. (*A*) Basal dendrite from a layer-5 pyramidal neuron, loaded with Alexa Fluor 488, in a mouse neocortical slice bathed in 2.5-mM MNI-glutamate. The red spots indicate the sites of simultaneous two-photon uncaging of glutamate using an SLM. First, an image (*A*), of the dendritic spines selected to be activated, was acquired with galvanometer raster scanning. Second, a bitmap file (*B*) was generated with the uncaging locations selected in (*A*). Next, a Fourier transform of the image was set as the command to generate a phase mask and the desired diffraction pattern, in this case, five uncaging spots next to spine heads (*A*). The voltage responses triggered after uncaging glutamate right next to the spine heads were recorded with a whole-cell patch-clamp recording electrode from the cell somata (*C*). Five (out of 15) representative uncaging potentials are depicted here. These were generated after simultaneously uncaging glutamate right next to the spine heads shown in (*A*). (*D*) Average of 15 uncaging potentials (including the ones in *C*). The black trace is the average uncaging potential as shown in *D*. Light gray in *D* is ±SEM. (Modified, with permission, from Nikolenko et al. 2008.)

caged-L-glutamate (MNI-glutamate). The basal dendrites and selected arrays of dendritic spines from these pyramidal neurons were imaged with conventional raster scanning. The high-resolution images were used to compute phase masks targeting spines near the tips of their heads (Fig. 4). Next, five to 15 spines were simultaneously activated with the SLM phase masks, generating reliable uncaging potentials with fast kinetics (Nikolenko et al. 2008). Using SLM microscopy to simultaneously stimulate multiple individual spines or dendritic locations could help address fundamental problems in dendritic biophysics such as integration of inputs (Cash and Yuste 1998; Araya et al. 2006a; Losonczy and Magee 2006). In principle, similar experiments could be performed at the circuit level by stimulating arrays of neurons (Nikolenko et al. 2007, 2008).

Two-Photon Imaging of Multiple Neurons

SLM microscopy can also be used for fast multifocal two-photon imaging, providing the potential for rapid deep-tissue imaging of multiple sites of interest. This method has been used to image activity-related calcium signals from neuronal populations (Fig. 5). Multiple neurons were identified as imaging targets (Fig. 5A) within brain slices loaded with the calcium indicator Fura-2-acetoxymethyl ester (Fura-2AM). The phase pattern generated from the coordinates of these cellular locations (Fig. 5B) was used to create the diffractive pattern of excitation light. The resultant fluorescence was imaged using an EMCCD camera (Fig. 5C).

In the experiment shown, one neuron was whole-cell-patched with 50-μM Fura-2 to approximate the dye concentration in other neurons, and varying numbers of action potentials were evoked in the patched neuron. Action potential-related fluorescence transients were faithfully reported, with single spikes clearly detectable (Fig. 5D).

It should be pointed out that there is no scanning in this imaging mode because all points of interest are continuously illuminated. Thus the maximum possible temporal resolution of the microscope is defined only by the frame rate of the detector. The practical temporal resolution is set by the time required to collect a single frame of sufficient signal to noise for the given experiment. We have found it possible to obtain good two-photon Ca^{2+} signals at rates as high as 60 frames/sec.

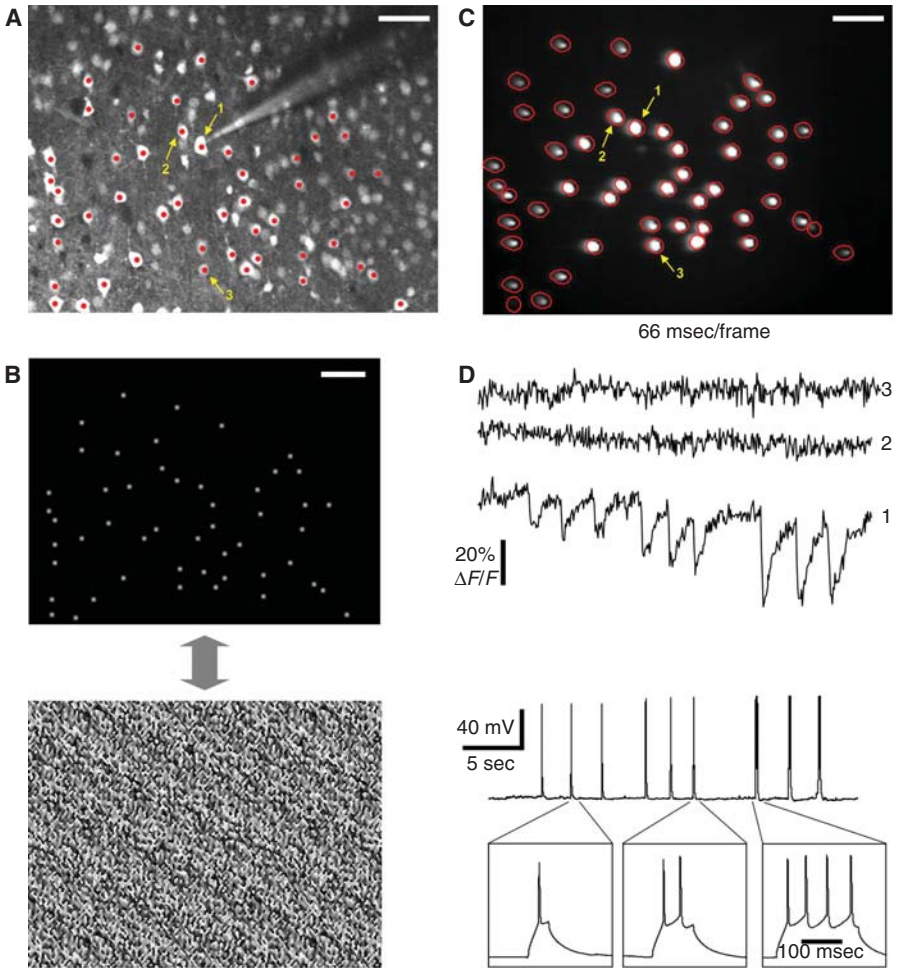

FIGURE 5. SLM multibeam imaging. (*A*) A neocortical slice (L2/3, area S1, P15 mouse) was bulk loaded with a Ca^{2+} indicator (a 10:1 mixture of Fura-2AM and mag-Indo-1AM [Nikolenko et al. 2007]). The image shown was taken using a standard two-photon raster imaging mode (790-nm excitation). Fifty neurons were targeted for imaging using a diffractive SLM (red spots). One of the neurons (labeled "1") was targeted for patch-clamp recording to trigger action potentials using current injection. The intracellular solution contained 50-μM Fura-2AM pentapotassium salt, a concentration that corresponds roughly to the intracellular concentration of Fura-2AM achieved by bulk loading (Peterlin et al. 2000). The pipette also contained 10-μM Alexa 594 for localization of the patched neuron using a different emission filter. (*B*) Command image file for SLM software and corresponding phase mask. (*C*) Image of two-photon fluorescence from multiple locations obtained with a camera. The diffractive SLM splits the laser beam to continuously illuminate spatially different locations with a static pattern (~4.4 mW of average excitation power per spot on the sample plane). Red contours were detected using custom software to quantify time-lapsed signals from different cells. Scale bar, 50 μm. (*D*) Calcium signals recorded from cells identified in (*A*) and (*C*) and corresponding to different numbers of action potentials elicited in cell 1 (nine current pulses that triggered triplets of one, two, and four action potentials, respectively, are shown). Even individual spikes can be detected with a good signal-to-noise ratio. Neurons 2 and 3 were not stimulated and did not show any change in fluorescent signals. Imaging was performed with ~15 frames/sec temporal resolution (66 msec/frame). No noticeable photobleaching or photodamage was observed over the course of the experiment (several minutes of continuous illumination). (Modified, with permission, from Nikolenko et al. 2008.)

CONCLUSION

A novel design of an optical microscope is presented based on an SLM that changes only the phase of light and redistributes the total available power among the points of interest. The utility of this approach is shown for simultaneous stimulation of multiple dendritic spines and neurons (Nikolenko et al. 2008) using two-photon uncaging of excitatory neurotransmitters. In addition, a new imaging paradigm has been designed that takes advantage of the selective illumination of the points of interest

 Cite this introduction as *Cold Spring Harb Protoc*; 2013; doi:10.1101/pdb.top079517

and combines it with fast imaging using a camera as the detector. This makes it possible to achieve high rates of signal acquisition not easily available with other nonlinear imaging techniques. The SLM microscope highlights some of the flexibility made available by this "universal" optic, and which could greatly simplify optical instrumentation and make it possible to construct miniaturized lightweight optical devices. This, in turn, could expand the utility of nonlinear imaging and photostimulation methods for a variety of in vivo and medical uses.

ACKNOWLEDGMENTS

We thank the National Eye Institute, the HHMI, and the Kavli Institute for funding, and we also thank the members of the Yuste laboratory for support and help.

REFERENCES

Araya R, Eisenthal KB, Yuste R. 2006a. Dendritic spines linearize the summation of excitatory potentials. *Proc Natl Acad Sci* **103:** 18799–18804.

Araya R, Jiang J, Eisenthal KB, Yuste R. 2006b. The spine neck filters membrane potentials. *Proc Natl Acad Sci* **103:** 17961–17966.

Araya R, Nikolenko V, Eisenthal KB, Yuste R. 2007. Sodium channels amplify spine potentials. *Proc Natl Acad Sci* **104:** 12347–12352.

Bauschke HH, Combettes PL, Luke DR. 2002. Phase retrieval, error reduction algorithm, and Fienup variants: A view from convex optimization. *J Opt Soc Am A* **19:** 1334–1345.

Cash S, Yuste R. 1998. Input summation by cultured pyramidal neurons is linear and position-independent. *J Neurosci* **18:** 10–15.

Hopt A, Neher E. 2001. Highly nonlinear photodamage in two-photon fluorescence microscopy. *Biophys J* **80:** 2029–2036.

Koester HJ, Baur D, Uhl R, Hell SW. 1999. Ca^{2+} fluorescence imaging with pico- and femtosecond two-photon excitation: Signal and photodamage. *Biophys J* **77:** 2226–2236.

Kuznetsova TI. 1988. On the phase retrieval problem in optics. *Sov Phys Usp* **31:** 364–371.

Losonczy A, Magee JC. 2006. Integrative properties of radial oblique dendrites in hippocampal CA1 pyramidal neurons. *Neuron* **50:** 291–307.

Lutz C, Otis TS, DeSars V, Charpak S, DiGregorio DA, Emiliani V. 2008. Holographic photolysis of caged neurotransmitters. *Nat Methods* **5:** 821–827.

Nikolenko V, Poskanzer KE, Yuste R. 2007. Two-photon photostimulation and imaging of neural circuits. *Nat Methods* **4:** 943–950.

Nikolenko V, Watson BO, Araya R, Woodruff A, Peterka DS, Yuste R. 2008. SLM microscopy: Scanless two-photon imaging and photostimulation with spatial light modulators. *Front Neural Circuits* **2:** 1–14.

Peterlin ZA, Kozloski J, Mao BQ, Tsiola A, Yuste R. 2000. Optical probing of neuronal circuits with calcium indicators. *Proc Natl Acad Sci* **97:** 3619–3624.

Wang S, Szobota S, Wang Y, Volgraf M, Liu Z, Sun C, Trauner D, Isacoff EY, Zhang X. 2007. All optical interface for parallel, remote, and spatiotemporal control of neuronal activity. *Nano Lett* **7:** 3859–3863.

Spatial Light Modulator Microscopy

Volodymyr Nikolenko, Darcy S. Peterka, Roberto Araya, Alan Woodruff and Rafael Yuste

Cold Spring Harb Protoc; doi: 10.1101/pdb.top079517